



Available online at [www.sciencedirect.com](http://www.sciencedirect.com)

**ScienceDirect**

Energy Reports 6 (2020) 275–285



[www.elsevier.com/locate/egyr](http://www.elsevier.com/locate/egyr)

Tmrees, EURACA, 25 to 27 June 2020, Athens, Greece

## Mitigating bed agglomeration in a fluidized bed gasifier operating on rice straw

Jurarat Nisamaneenate<sup>a</sup>, Duangduen Atong<sup>b</sup>, Anun Seemen<sup>a</sup>, Viboon Sricharoenchaikul<sup>a,c,\*</sup>

<sup>a</sup> Department of Environmental Engineering, Faculty of Engineering, Chulalongkorn University, Bangkok 10330, Thailand

<sup>b</sup> National Metal and Materials Technology Center, Thailand Science Park, Pathumthani 12120, Thailand

<sup>c</sup> Energy Research Institute, Chulalongkorn University, Bangkok 10330, Thailand

Received 2 August 2020; accepted 30 August 2020

### Abstract

Fluidized bed gasifier is a promising technology with respect to converting biomass to useful energy. Bed agglomeration is an operational challenge that arises during fluidized bed gasification with rice straw as raw materials. Rice straw contains high amounts of potassium and other components that may lower the melting point of ash, causing bed agglomeration. Using alternative bed materials such as alumina, in the place of silica, can mitigate this problem. In Thailand, rice straw is an agricultural by-product of the rice milling processes, produced in large quantities every year. Usually, rice straw management comprises open field burning, which releases greenhouse gases, particulate matter, and other pollutants. In this paper, the behaviors of bed agglomeration and defluidization were investigated during the fluidized bed gasification of rice straw, using silica and alumina as bed materials. The effect of the percentage ratio of silica and alumina (0:100; 25:75; 50:50; 75:25; 100:0) was examined. The operating parameters were as follows: rice straw particle size of 425–850  $\mu\text{m}$ , reaction temperature of 700–900  $^{\circ}\text{C}$ , and equivalence ratios (ER) of 0.2 and 0.4. The results showed that the percentage ratio of silica and alumina, 0:100 at 700  $^{\circ}\text{C}$ , had extended the defluidization time of 60 min. The effect of equivalence ratio on bed agglomeration was found to be apparently heightened at a high temperature. The result of SEM/EDX analysis showed that the major elements at the linkage point of the agglomerated particle were Si, K, and Ca, with regard to any proportion of the alumina bed and temperature. In conclusion, low temperature agglomerate formation can be explained by a  $\text{K}_2\text{O}-\text{CaO}-\text{Si}_2\text{O}$  phase diagram. The results from this investigation can be applied to biomass-fluidized bed gasification, where bed agglomeration entails a plant shutdown and is expensive in terms of maintenance.

© 2020 The Authors. Published by Elsevier Ltd. This is an open access article under the CC BY-NC-ND license (<http://creativecommons.org/licenses/by-nc-nd/4.0/>).

Peer-review under responsibility of the scientific committee of the Tmrees, EURACA, 2020.

**Keywords:** Alkali; Biomass; Defluidization; Gasification; Renewable energy

### 1. Introduction

Renewable energy is mostly studied by researchers around the world in relation to the driving force of energy demand. Biomass is intriguing renewable energy due to high potential intrinsic energy when compared with other

\* Corresponding author at: Department of Environmental Engineering, Faculty of Engineering, Chulalongkorn University, Bangkok 10330, Thailand.

E-mail address: [viboon.sr@chula.ac.th](mailto:viboon.sr@chula.ac.th) (V. Sricharoenchaikul).

<https://doi.org/10.1016/j.egyr.2020.08.050>

2352-4847/© 2020 The Authors. Published by Elsevier Ltd. This is an open access article under the CC BY-NC-ND license (<http://creativecommons.org/licenses/by-nc-nd/4.0/>).

Peer-review under responsibility of the scientific committee of the Tmrees, EURACA, 2020.

traditional renewable energy sources [1]. Biomass is not only obtained from any plant but also from agriculture residue, such as rice straw, woodchip, peanut shell, corn cob and bagasse. Thailand is an agricultural country, and therefore it is witnessing growing trend steered towards the use of biomass-based energy. In general, most agriculture residues are dumped or burnt in open air, generating pollutants including dust, NO<sub>x</sub>, and SO<sub>x</sub>. As Thailand is a major rice exporting country, there are abundant amounts of rice straw gathered after the harvesting season [2]. The proper management of rice straw are needed to avoid air pollution caused by the open field burning. However, it has a high heating value and its residues have immense potential to generate fuel and energy [3]. Normally, biomass can be converted into energy and other chemicals products via thermochemical processes. Combustion, pyrolysis, and gasification are the three main thermochemical conversion methods [4]. A fluidized bed is widely used for the combustion of biomass because it is suitable for low-grade material fuels. As a result of its highly efficient heat transfer, excellent gas–solid contact, and temperature distribution in the reactor [5,6], the fluidized bed gasifier is a promising technology with respect to converting biomass to renewable energy. Several researches have been performed on the thermochemical conversion via gasification and combustion processes of rice straw [7–10]. Nevertheless, bed agglomeration might lead to limitation in the fluidization of rice straw. Indeed, bed materials are crucial to fluidized bed gasifiers. The fluidized combustion of biomass fuels is associated with a high possibility of agglomeration when one uses conventional bed materials [11]. This is due to chemical components in the rice straw which consists of inorganic alkalis such as calcium, potassium, and sodium. The bed agglomeration is attributed to the presence of alkaline species in the biomass. During the fluidization process, alkalis can be a source of the abovementioned problem by forming low-melting silicates with the silica from the sand; this leads to bed agglomeration and clogging, lead to the unscheduled shutdown of the affected plant. The alkaline species in ash can be transferred to the surface of the bed and facilitate the formation of a coating layer during combustion and gasification [12–16]). To mitigate this problem, alternative bed materials such as calcite and alumina can be used in place of silica. Until now, very few researches have addressed the gasification of rice straw using a fluidized silica–alumina bed. The used of alumina based bed materials may mitigate agglomeration problem in fluidized bed gasification thus providing fuel flexibility and extended defluidization time. Although alumina has a promising potential to effectively decrease bed agglomeration, it is more costly when compared to silica sand. Thus, it should be reasonable used to lessen the cost and increase the efficiency of biomass conversion.

The objective of the present work is to study the bed agglomeration during the fluidized bed gasification of rice straw. The effect of the silica to alumina ratio was evaluated as well as the influences of ER and temperature on the defluidization time and bed agglomeration. SEM/EDS techniques would be employed on surface, necks and cross section of spent bed materials to allow in depth understanding of the chemistry behind this phenomenon which would lead to selection of optimal operating conditions for prevention of bed agglomeration and thus reduction of otherwise costly regular maintenance.

## 2. Materials and methods

### 2.1. Materials

The biomass used was rice straw, an agriculture by-product abundantly available in central Thailand. Rice straw was fed to the crusher, and thereafter sieved out to targeted size between 425 to 850  $\mu\text{m}$ . The alumina (250–425  $\mu\text{m}$ ) and silica sand (425–500  $\mu\text{m}$ ) are bed materials used for the experiment. The solid densities of the bed materials were rather different: 3620  $\text{kg}/\text{cm}^3$  for alumina and 2600  $\text{kg}/\text{cm}^3$  for silica sand. Both the proximate and ultimate analyses of the rice straw utilized in this research's gasification experiments are reported in Table 1. The rice straw contained large volatile organic content and low fixed carbon; a high carbon and low nitrogen content, suitable for thermal conversion with a lowered degree of environmental pollution. The compositions of raw materials and bed materials are shown in Table 2. The main components of material were SiO<sub>2</sub> (60.30%), K<sub>2</sub>O (18.46%), and CaO (7.62%), which resulted in their accumulation between the biomass and the bed (in the fluidization system) during the experiment.

### 2.2. Experimental setup and procedure

Gasification experiments were conducted in the abovementioned fluidized bed gasification system. As per the information that was obtained, the reactor was composed of high-temperature stainless steel. The reactor's total

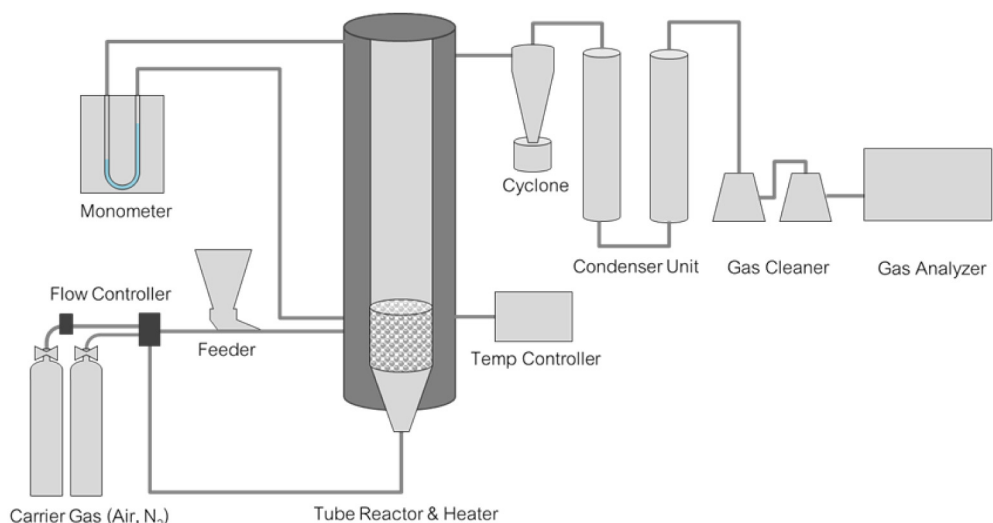
**Table 1.** Characteristics of raw material.

Proximate Analysis (wt.%)		Rice Straw
Moisture		9.30
Ash		11.84
Volatile organic content		66.56
Fixed carbon		12.31
LHV, (MJ/Kg)		16.09
Ultimate Analysis (wt.%)		
Carbon		44.00
Hydrogen		7.64
Nitrogen		0.11
Sulfur		0.00
Oxygen <sup>a</sup>		48.25
Physical Properties:		
Bulk density (kg/m <sup>3</sup> )		160.63

<sup>a</sup>By difference.**Table 2.** Compositions of raw material and bed material.

Inorganic (% wt.)	SiO <sub>2</sub>	Al <sub>2</sub> O <sub>3</sub>	K <sub>2</sub> O	CaO	Na <sub>2</sub> O	MgO	P <sub>2</sub> O <sub>5</sub>	Fe <sub>2</sub> O <sub>3</sub>	TiO <sub>2</sub>	Others
Rice straw	60.30	0.24	18.46	7.62	1.82	1.56	1.02	—	—	8.98
Silica	99.47	0.08	—	0.08	0.10	—	—	0.03	0.14	0.10
Al <sub>2</sub> O <sub>3</sub>	0.10	98.70	—	0.04	0.36	—	—	0.08	0.00	0.72

height was 100 cm with respect to the lower section (conical), while inner diameter was 5 cm. The lower section contained a perforated steel plate distributor of 5 cm thickness and in a 40° angle. The system consisted of a feeder, gasifier, heater furnace, cyclone, condenser unit, gas cleaner, and gas analyzer, as shown in Fig. 1. The reactor was located in an electrical furnace which controlled by proportional integral derivative (PID) regulator. A thermocouple (K-type) was placed above the plate distributor to measure bed temperature. Manometer was used to measure the pressure drop for monitoring the bed agglomeration progress. In addition, the cyclone and the condenser were used to clean the evolved gas product before being analyzed by gas analyzer (real-time) [7,15,17].

**Fig. 1.** Schematic of fluidized bed gasification system.

The experiment commenced with heating up the reactor by an electrical furnace to the desired operating temperature. Through the heating process, the carrier gas was fed into the reactor continuously with the use of a rotameter to controlled feeding rate. At the set point operating temperature, the trial was initiated by the feeding of the mixed air/nitrogen and straw (4 g/min) into the reactor. Bed agglomeration were continuously monitored by detecting changes in the pressure drop across the bed. Prior to gas sampling by an online gas analyzer, the particulates and condensable species in the gaseous product were trapped. The experiment was halted when the pressure sharply dropped. In this study, defluidization time was defined as the time between the start of the straw feeding and the termination of the experiment via defluidization.

### 2.3. Characterization of agglomerates

After fluidized bed gasification tests, samples of the silica and alumina bed were collected and investigated using a scanning electron microscope (SEM, Hitachi SU5000, Japan) in order to obtain a clear view of the reactions between the ash-forming elements and the agglomerated parts [8,15,18]. This technique was employed on surface, necks and cross section of spent bed materials to allow an understanding of the chemistry behind this phenomenon.

## 3. Results and discussion

### 3.1. Effect of gasification

The defluidization of silica sand during fluidized bed combustion and the gasification of rice straw can be identified by a pronounced and sudden accompanying pressure decrease across the bed. Fig. 2 shows the point through a time series of pressure drop between the freeboard of the reactor and above the upper-stage distributor. During system startup, the pressure drop suddenly decreased under combustion-oriented conditions at 700 °C. When the temperature increased to 800 °C, the pressure drop decreased after three minutes. In the case of fluidized bed gasification, the pressure drop slightly decreased under gasification conditions at 700 °C and 800 °C. Conditions such as the baseline of the bed pressure decreased until complete defluidization was achieved after 40 min. In their gaseous alkali phases, the inorganic components of rice straw, such as calcium and potassium, can react with oxygen to produce oxide composition. Reactions of calcium oxide can take place at a temperature of over 300 °C in air [19] which leads to bed agglomeration and clogging, resulting in the bed pressure decreased. Thus, the gasification process can reduce bed material accumulation and extend the defluidization time.

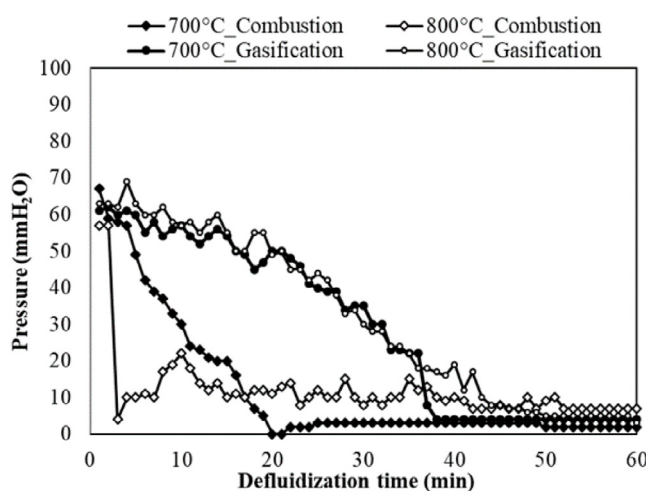


Fig. 2. Pressure profiles along the agglomeration.

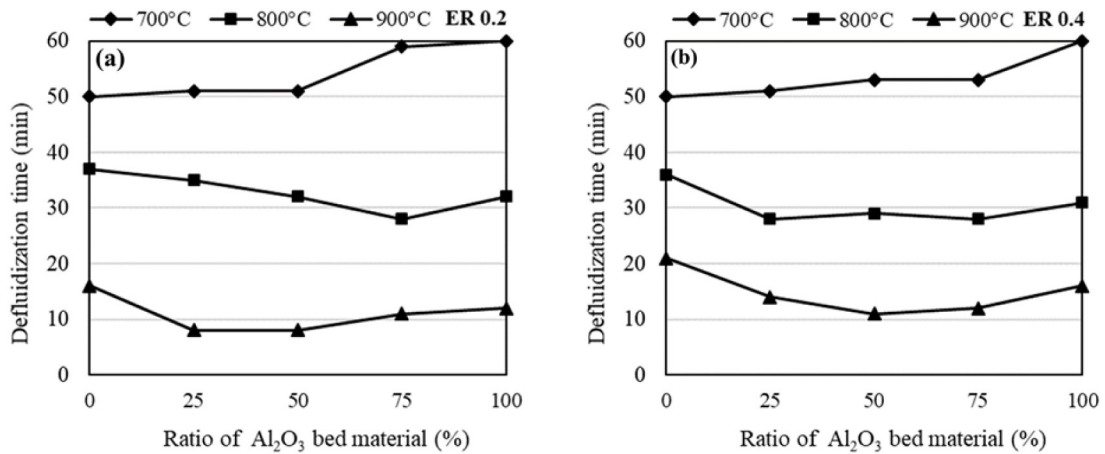


Fig. 3. Effect of  $\text{Al}_2\text{O}_3$  ratio on bed agglomeration.

### 3.2. Effect of bed Temperature and the ratio of silica to alumina

One of the most important parameters effecting all the chemical reactions involved in fluidized bed gasification is bed temperature. The effect of bed temperature on this experiment was investigated within the range of 700–900 °C. The air flow rate was varied from 1.77 to 2.03  $\text{m}^3/\text{hr}$ , depending on the temperature and the equivalent ratio. The results of ER 0.2 are shown in Fig. 3(a). Under the 700 °C test condition, the range of the defluidization time was 50–60 min for all ratios. Meanwhile, the range of the defluidization time was measured as 30–40 min at 800 °C, whereas for 900 °C the range of the defluidization time decreased to 10–20 min. In case of the ER 0.4 test conditions, the results show that when the temperature was increased from 700 °C to 900 °C, the defluidization times for all ratios decreased. The range of the defluidization time was 53–60 min, 28–36 min, and 11–21 min at 700 °C, 800 °C, and 900 °C, respectively, as shown in Fig. 3(b). The results of this test showed that the effect of reaction temperature on defluidization time is significant; with an increase in the temperature, the defluidization time decreased. From the experiment results, the melting of a low-liquid substance ( $\text{K}_2\text{O}-\text{CaO}-\text{SiO}_2$ ) was observed. This substance is viscous and can be bonded to the surface of bed particles. Causing the bed to accumulate when collisions between bed particles. In this vein, Yu et al. [10] conducted bed accumulation after a fluidized bed combustion of rice straw by using silica at temperatures of 650–910 °C. The authors found that increasing the temperature caused the defluidization time of the bed to decrease.

Even after increasing the ratio of  $\text{Al}_2\text{O}_3$  from 0% to 50% at 700 °C, the defluidization times were found to remain quite stable at approximately 50 min. Also, the defluidization times expanded to 60 min with 100% ratios of  $\text{Al}_2\text{O}_3$ . The results showed that increasing the alumina ratio led to an extension of the defluidization time. Due to the high alumina and low silica content in the bed, this reduced the substances of a low melting point  $\text{K}_2\text{O}-\text{CaO}-\text{SiO}_2$ . Thus, the authors asserted that high  $\text{Al}_2\text{O}_3$  percentages can help reduce the effect of the agglomeration potential on the eutectic melting point of ternary mixtures, such as  $\text{SiO}_2-\text{CaO}-\text{K}_2\text{O}$ . The formation of the  $\text{SiO}_2-\text{CaO}-\text{K}_2\text{O}$  mixture with a low eutectic melting point was associated with a temperature of 710 °C [18]. This eutectic formation occurred in the bed with a high ratio of silica sand. As a result, both 75% and 100% of  $\text{Al}_2\text{O}_3$  can prolong the defluidization time. Indeed, increasing ratios of  $\text{Al}_2\text{O}_3$  can extend the defluidization time, due to the formation of  $\text{SiO}_2-\text{Al}_2\text{O}_3-\text{K}_2\text{O}$  mixture with low eutectic melting point at 750 °C [20]. Therefore, the molten ash obtained may form linkages between  $\text{Al}_2\text{O}_3$  beds. Theoretically, the formations of  $\text{SiO}_2-\text{CaO}-\text{K}_2\text{O}$  and  $\text{SiO}_2-\text{CaO}-\text{Na}_2\text{O}$  mixtures can occur in the presence of 25%–75%  $\text{Al}_2\text{O}_3$ , because of their low eutectic melting points at 710 °C and 725 °C, respectively.

From Fig. 3, it can be observed that at 800 °C and 900 °C, similar trends are shown. The increasing ratios of  $\text{Al}_2\text{O}_3$  result in the defluidization time being decreased. At temperatures over 750 °C, the bed containing silica and alumina can form low-melting-point substances, such as  $\text{K}_2\text{O}-\text{CaO}-\text{SiO}_2$  and  $\text{K}_2\text{O}-\text{Al}_2\text{O}_3-\text{SiO}_2$ , resulting in a shorter fluidization time while the ratio of alumina increases. Moreover, applying 100% ratios of  $\text{Al}_2\text{O}_3$  at the

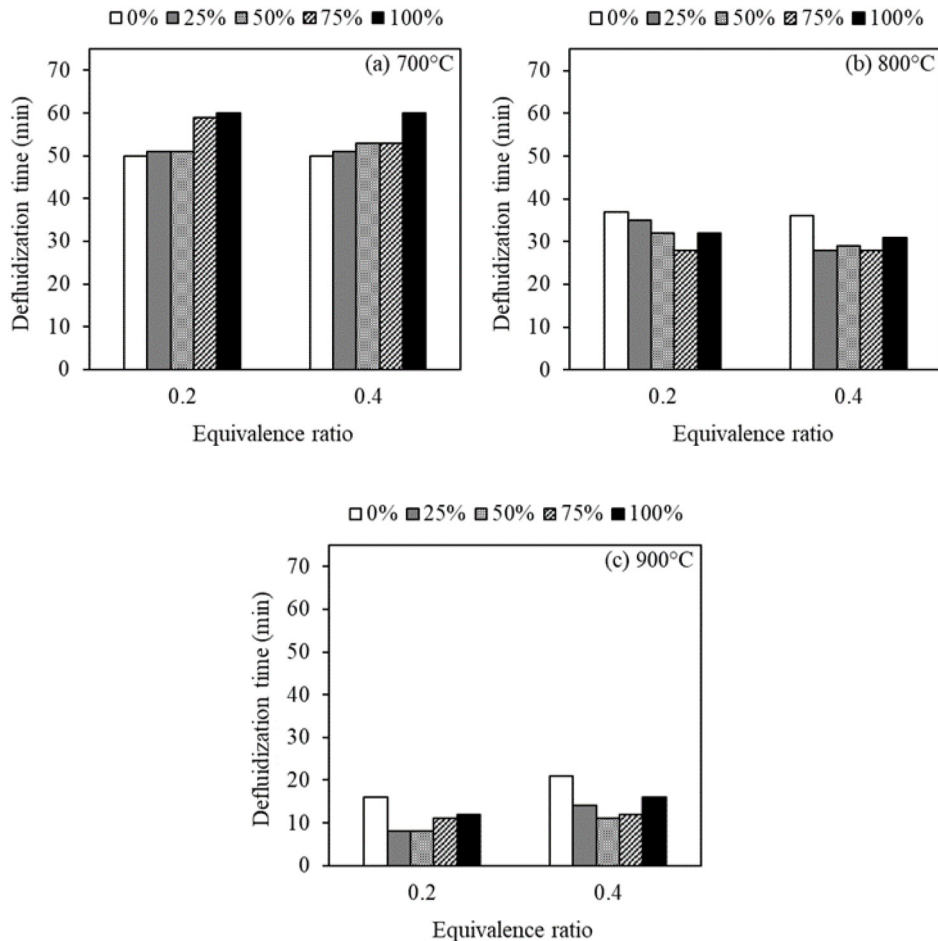


**Fig. 4.** Effect of ER on bed agglomeration in relation to Al<sub>2</sub>O<sub>3</sub> ratio at (a) 700 °C; (b) 800 °C; and (c) 900 °C.

same temperature would slightly increase defluidization time. Since the bed does not contain silica, the possibility of K<sub>2</sub>O–CaO–SiO<sub>2</sub> compound being formed, which causes bed accumulation, decreases. This result was found to be similar to the trend of defluidization time with respect to the fluidized bed combustion of rice straw at 750 °C [10]. The influence of temperature on defluidization time was found to have significantly decreased, which implied a more pronounced effect of reaction temperature on bed agglomeration than that of the Al<sub>2</sub>O<sub>3</sub> ratio.

### 3.3. Effect of equivalence ratio

Fig. 4(a–c) show the effects of equivalence ratio on bed accumulation. The effect of the equivalence ratio on fluidized bed gasification was studied at 0.2 and 0.4. At 700 °C, the defluidization time in relation to Al<sub>2</sub>O<sub>3</sub> ratios of 0%, 25%, and 100% was 50 min, 51 min, and 60 min, respectively, with both the equivalent ratios. While the defluidization time related to the 50% Al<sub>2</sub>O<sub>3</sub> ratio, with an equivalent ratio 0.4, was higher than the equivalent ratio 0.2, with respect to a 75% Al<sub>2</sub>O<sub>3</sub> ratio the defluidization time of the equivalent ratio 0.2 was found to be greater than that with an equivalent ratio of 0.4. At 800 °C, the defluidization time with 0%, 25%, and 100% Al<sub>2</sub>O<sub>3</sub> ratios, in terms of the equivalent ratio 0.2, were found to be higher than the equivalent ratio 0.4. In contrast, the defluidization time with 75% of Al<sub>2</sub>O<sub>3</sub> ratio (at the equivalent ratio 0.2) was higher than the equivalent ratio 0.4. For the 50% Al<sub>2</sub>O<sub>3</sub> ratio, the defluidization time was measured as 28 min with both the above equivalent ratios. At 900 °C, ranges of defluidization time was 10–20 min with both equivalent ratios. From the experiment results, the defluidization times from 700 °C, 800 °C, and 900 °C, with respect to equivalent ratios (0.2 and 0.4), were not

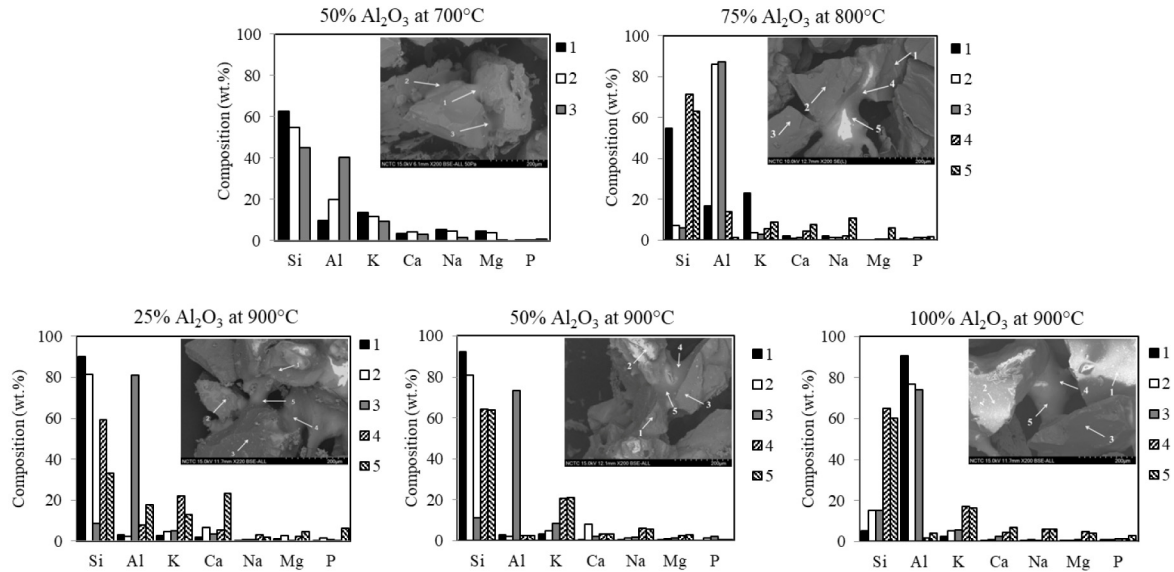


Fig. 5. SEM micrograph and EDS analysis of bed agglomeration (ER 0.2).

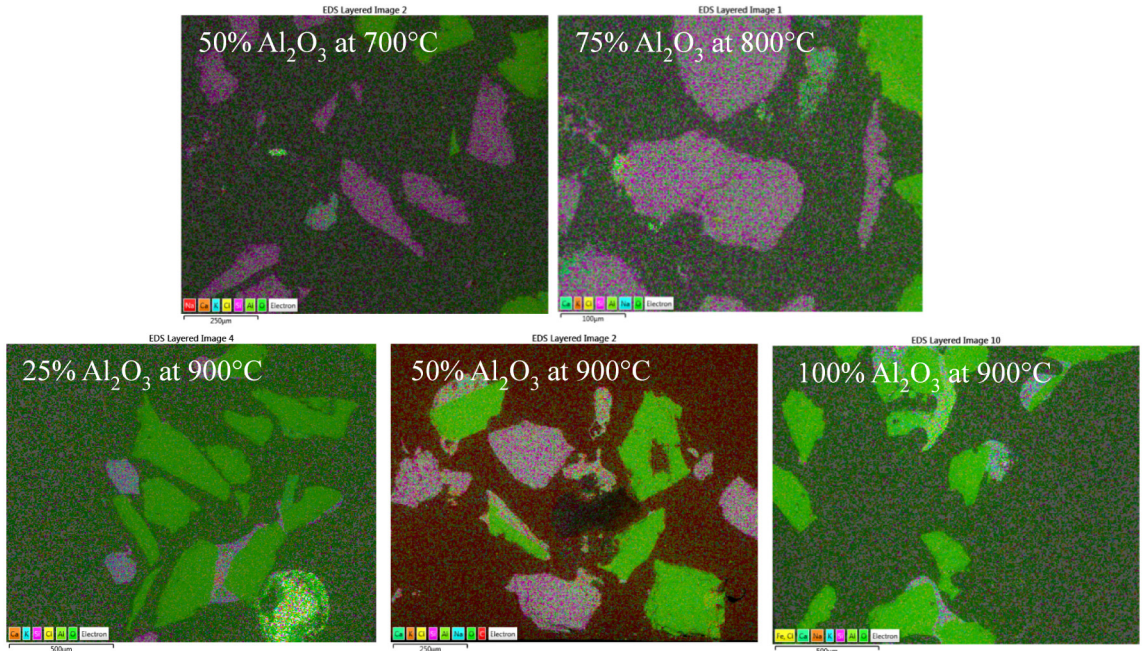


Fig. 6. Cross-sectional SEM micrograph of bed agglomeration (ER 0.2).

significantly different at the level of 0.05. Thus, the equivalence ratio at 0.2 is suitable for fluidized bed gasification of rice straw in terms of the defluidization time and quality of gas [21].

### 3.4. Characteristics of agglomerates

This research studied agglomerated beds during the gasification process completed by SEM/EDS. The cross-section, surface, and elemental composition of coatings and necks by EDS are shown in Figs. 5 and 6. Their

numberings showed the exact locations on the bed where they were analyzed in light of the elemental composition of coatings and necks. The bar graph showed elemental composition at each point on the surface of the agglomerated bed, as related to the SEM images under the same conditions. The main elements at the neck (linkage) point were Si, K, and Al in case of a 50%  $\text{Al}_2\text{O}_3$  bed at 700 °C, while the minor elements of Ca, Na, and Mg are shown in Fig. 5. The Si and  $\text{Al}_2\text{O}_3$  beds did not melt or get diffused inside the bed, as shown in the figure containing a cross-section of the bed (Fig. 6). In case of 75%  $\text{Al}_2\text{O}_3$  at 800 °C (Fig. 5), points 1, 2, and 3 present the bed surface area, whereas points 4 and 5 present the coatings and the necks of the bed. From the EDS, point 1 was found to contain high amounts of Si and K. It was expected that the surface of the silica bed particles was composed by the coating of the  $\text{K}_2\text{O}-\text{CaO}-\text{SiO}_2$  mixture, whose melting point was below 800 °C. These substances coated only the surface of the bed, as shown in Fig. 6. Points 2 and 3 displayed an abundance of  $\text{Al}_2\text{O}_3$ , which probably covered the surface area of the alumina bed. At points 4 and 5, the linkages of the bed had high Si and K and low Ca, Na, and Mg contents, respectively, which are the main components of ash derived from rice straw. The XRF analysis of the rice straw clearly shows high amounts of  $\text{SiO}_2$ ,  $\text{K}_2\text{O}$ ,  $\text{CaO}$ ,  $\text{Na}_2\text{O}$ , and  $\text{MgO}$  (Table 2). These components can accelerate bed agglomeration by forming eutectic mixtures of  $\text{K}_2\text{O}-\text{CaO}-\text{SiO}_2$  and  $\text{SiO}_2-\text{Al}_2\text{O}_3-\text{K}_2\text{O}$ , which facilitates the adhesion of bed particles. At 800 °C, the melting temperature behaviors related to linkage were observed between 720–740 °C.

The morphologies of coating and neck from experiments run with 25% and 50%  $\text{Al}_2\text{O}_3$  at 900 °C is revealed in Figs. 5 and 6. Evidently, these morphologies had a high amount of Si and a small amount of K at points 1 and 2. This indicated that the surface of the silica bed was coated with small amounts of low-melting-point mixtures. Point 3 had a high alumina content along with fewer degrees of other components as well. Points 4 and 5 had high amounts of Si and K, which can form low-melting-point compositions. With respect to the highest alumina ratio (100%) at points 1, 2 and 3, the surface area of alumina was marked by a high composition of Al and lowered presences of Si and K, while points 4 and 5 also presented high Si, followed by K, Ca, Na, and Mg, respectively. In Fig. 6, the cross sections of some  $\text{Al}_2\text{O}_3$  beds were bound together at the surface and the neck of contact via adhesive materials mainly composed of Si, Ca, and K. The formations of  $\text{K}_2\text{O}-\text{CaO}-\text{SiO}_2$  eutectics were not observed inside the bed. Moreover, at a high temperature we confirmed that the adhesive used as the bed material involves silica and alumina agglomeration by delving into a cross-sectional view.

As for the melting behaviors of neck at 900 °C from 25%  $\text{Al}_2\text{O}_3$ , the composition of the  $\text{K}_2\text{O}-\text{CaO}-\text{SiO}_2$  system had a melting range of 740–825 °C [18]. Moreover, both 50% and 100%  $\text{Al}_2\text{O}_3$  at the same temperature produced two melting point behaviors: between 740–825 °C for the  $\text{K}_2\text{O}-\text{CaO}-\text{SiO}_2$  system and 710–725 °C for  $\text{K}_2\text{O}-\text{Al}_2\text{O}_3-\text{SiO}_2$  [20]. As the results suggest, the melting point of  $\text{K}_2\text{O}-\text{CaO}-\text{SiO}_2$  may come to the fore even while using 100%  $\text{Al}_2\text{O}_3$ , because the ash content in rice straw can lead to the formation of low-melting-point mixtures with Si, K, and Ca. Hence, the bed agglomeration was exhibited in the experiments with 100%  $\text{Al}_2\text{O}_3$  at 800 °C and 900 °C. The  $\text{Al}_2\text{O}_3$  bed could be directly used as bed material or as a bed additive to effectively reduce the potential of bed agglomeration under optimum temperature [5].

The morphology of bed with respect to the effect of the equivalent ratio test at 0.4 is shown in Fig. 7. In case of 50%  $\text{Al}_2\text{O}_3$  at 700 °C, Fig. 7(a, b), points 1 and 2 contained silica at the surface. They also had high Si contents along with small amounts of K, Ca, Na, and Mg. Here, one can expect that the surface of the silica particles is coated with a molten material constituted by low melting points substances. Meanwhile, the surfaces of alumina at points 4 and 5 had high Al content and lower Si, K, and Ca contents. The neck (linkage) point revealed a similar composition of silica surfaces at points 6 and 7. The results obtained with respect to 75%  $\text{Al}_2\text{O}_3$  at 800 °C are depicted Fig. 7(c, d). Point 1 had a high amount of Si and small amounts of K and Ca, while points 2 and 3 had high amounts of Al as well as small amounts of Si, K, and Ca. Moreover, point 2 was found to have a high degree of Mg, probably because of the ash from the rice straw present at the surface area of alumina. The linkage points displayed Si, K, and Ca at points 4 and 5. The cross section in Fig. 7(c) can be classified into melt-induced agglomeration, which involves molten of ash particles with bed material [12].

From the results of the bed studied above, it can be agglomerated in relation to all temperatures and all the alumina ratios owing to the melting point of  $\text{K}_2\text{O}-\text{CaO}-\text{SiO}_2$ , which can melt at a temperature higher 720 °C, composed by  $\text{SiO}_2$ ,  $\text{K}_2\text{O}$ , and  $\text{CaO}$  that are obtained from ash-containing rice straw. When the temperature is increased, the K content decreases at the surfaces of the silica bed particles. In addition, at the alumina surfaces contained small amounts of K at both low and high temperatures. It can be concluded that the main reason behind bed agglomeration associated with the fluidized bed gasification of rice straw is melt-induced, which entails collisions between the bed particles and the molten ash particles. Still, the coating-induced agglomeration of the molten substance on the surface of bed was hardly affected.

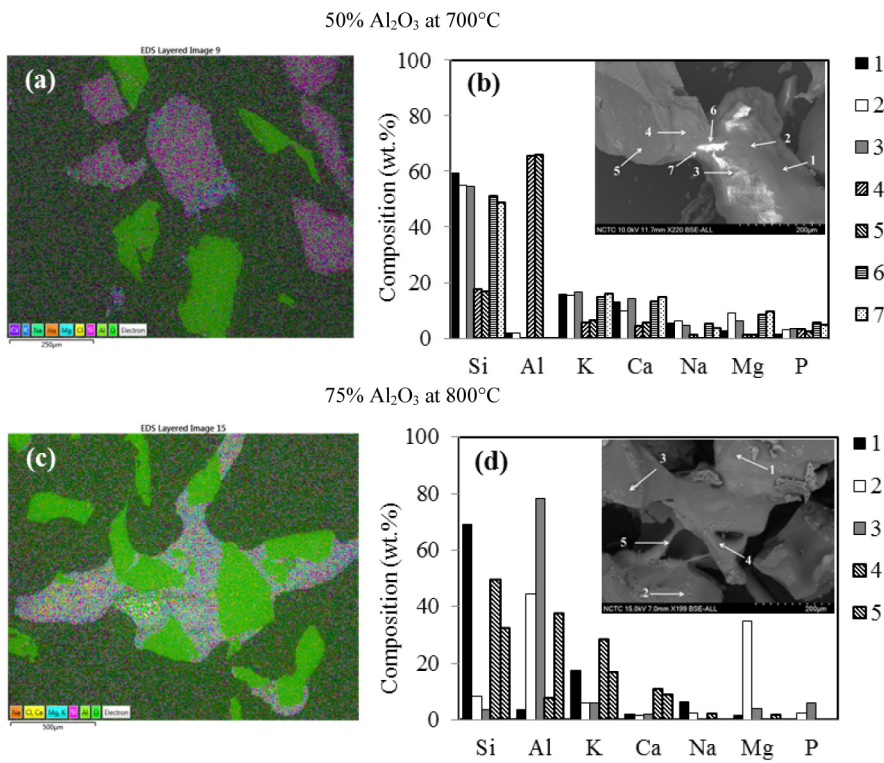


**Fig. 7.** SEM micrograph and EDS analysis of bed agglomerated (ER 0.4).

**Table 3.** Fuel gas composition.

Component	Carbon or Hydrogen Conversion %	
ER	0.2	0.4
H <sub>2</sub>	5–17	7–11
CO	24–34	24–33
CO <sub>2</sub>	11–30	19–32
C–CH <sub>4</sub>	8–11	8–11
H–CH <sub>4</sub>	15–21	14–21

### 3.5. Syngas composition

Hydrogen and carbon conversions at all alumina ratios are displayed in [Table 3](#). The production gas obtained from this experiment mainly consisted of CO, CO<sub>2</sub>, H<sub>2</sub>, and CH<sub>4</sub>, and a higher temperature led to a greater degree of CO and H<sub>2</sub> conversion. The results of the ER 0.2 test showed that the conversion of carbon to CO was in the range 24%–34%. The conversion of carbon to CO<sub>2</sub> was 11%–30%. The carbon conversion to CH<sub>4</sub> was 8%–11%. The hydrogen conversion to H<sub>2</sub> and CH<sub>4</sub> was 5%–17% and 15%–21%, respectively. For the equivalent ratio 0.4, the conversion of hydrogen to H<sub>2</sub> gas was lower than that in ER 0.2, besides the conversion of carbon to CO<sub>2</sub> being higher than that in ER 0.2. The increased amount of oxygen reacting with the carbon present in the raw material, along with other chemical reactions, produced CO<sub>2</sub>. The generated CO<sub>2</sub> was consumed by the water–gas reaction to yield more CO<sub>2</sub> [1], whose effect on the quality of gas production (in terms of heating value) decreased. Several studies in both bubbling fluidized bed and downdraft fixed bed gasification of biomass such as empty palm fruit bunch and peanut shell waste reported that at a high ER, more oxygen is supplied into the gasifier, and a high temperature enhances the production of CO<sub>2</sub> via char burning [17,22]. The fuel gas obtained in this experiment can be used in engines, steam turbines, as well as in other processes.

#### 4. Conclusions

In this research, the temperature was found to have affected bed agglomeration. Increasing the temperature in this experiment resulted in a faster bed agglomeration. The operating temperature was higher than the melting point temperature of the  $K_2O-CaO-SiO_2$  and  $K_2O-Al_2O_3-SiO_2$  mixtures. Hence, regarding the effect of the proportion of silica to alumina in the bed behaviors, the results indicated that increasing the ratio of alumina yielded an increase in the defluidization time at low temperatures. On the other hand, at higher temperatures, the defluidization time was found to have decreased. Therefore, a reaction temperature lower than 700 °C can prolong defluidization time. Equivalent ratios also affect the bed agglomerations associated with gasification processes. When considered together with temperature, at low temperatures the equivalent ratio does not affect defluidization time. The product gas obtained from this experiment was found to be mainly composed by CO, CO<sub>2</sub>, H<sub>2</sub>, and CH<sub>4</sub>. This fuel gas can be applied to engines, steam turbines as well as other relevant processes. To summarize, the results of this research can be used to improve the existing fluidized bed gasification processes by maintaining the fluidized bed conditions and reducing the occurrences of bed agglomeration. Moreover, it can also be applied in industries such as biomass power plants, where it can help reduce the instances of plant shutdown as well as reduce related costs of repair and maintenance systems.

#### Declaration of competing interest

The authors declare that they have no known competing financial interests or personal relationships that could have appeared to influence the work reported in this paper.

#### Acknowledgments

This research project is supported by the Second Century Fund (C2F), Chulalongkorn University, Thailand. Authors would like to thank the Department of Environmental Engineering, Faculty of Engineering, Chulalongkorn University and National Metal and Materials Technology Center for their assistance on material analysis and laboratory space.

#### References

- [1] Knoef HAM. *Handbook biomass gasification*. 2nd ed. Enschede: Biomass Technology Group BV; 2012.
- [2] Office of agricultural economics [Internet]. 2019, Available from: [www.oae.go.th](http://www.oae.go.th), [cited 24 2019].
- [3] Gadde Butchaiah, Menke Christoph, Wassmann Reiner. Rice straw as a renewable energy source in India, Thailand, and the Philippines: Overall potential and limitations for energy contribution and greenhouse gas mitigation. *Biomass Bioenergy* 2009;33(2009):1532–46.
- [4] Basu Prabir. Gasification theory and modeling of gasifiers. In: Basu P, editor. *Biomass gasification and pyrolysis*. Boston: Academic Press; 2010 [Chapter 5].
- [5] Basu Prabir. Combustion and gasification in fluidized beds. Taylor & Francis Group, LLC.; 2006.
- [6] Alauddin Zainal Alimuddin Bin Zainal, Lahijani Pooya, Mohammadi Maedeh, Mohamed Abdul Rahman. Gasification of lignocellulosic biomass in fluidized beds for renewable energy development: A review. *Renew Sustain Energy Rev* 2010;14(9):2852–62.
- [7] Calvo Luis Fernando, Gil María Victoria, Otero Marta, Morán A, García Ana Isabel. Gasification of rice straw in a fluidized-bed gasifier for syngas application in close-coupled boiler-gasifier systems. *Bioresour Technol* 2012;109:206–14.
- [8] Chaivatamaset Pawin, Sricharoon Panchan, Tia Suvit, Bilitewski Bernd. The characteristics of bed agglomeration/defluidization in fluidized bed firing palm fruit bunch and rice straw. *Appl Therm Eng* 2014;70(1):737–47.
- [9] Liu Huanpeng, Feng Yujie, Wu Shaohua, Liu Dunyu. The role of ash particles in the bed agglomeration during the fluidized bed combustion of rice straw. *Bioresour Technol* 2009;100(24):6505–13.
- [10] Yu Chuanjiang, Qin Jianguang, Nie Hu, Fang Mengxiang, Luo Zhongyang. Experimental research on agglomeration in straw-fired fluidized beds. *Appl Energy* 2011;88(12):4534–43.
- [11] Yang Wen-ching. *Handbook of fluidization and fluid-particle systems*. New York: Dekker; 2003.
- [12] Visser HJM. The influence of fuel composition on agglomeration behaviour in fluidised-bed combustion. Delft: Energy Research Centre of the Netherlands ECN; 2004.
- [13] Unchaisri Thanet, Fukuda Suneerat. Co-firing of coal and rice straw pellet in a circulating fluidized-bed reactor. *Energy Procedia* 2017;138(2017):766–71.
- [14] Shimizu Tadaaki, Han Jun, Choi Sunyong, Kim Laehyun, Kim Heejoon. Fluidized-bed combustion characteristics of cedar pellets by using an alternative bed material. *Energy Fuels* 2006;20(6):2737–42.
- [15] Fryda Lydia, Panopoulos Kyriakos D, Kakaras Emmanouil. Agglomeration in fluidised bed gasification of biomass. *Powder Technol* 2008;181:307–20.

- [16] Rozainee Mohd, Ngo Saik Peng, Salema Arshad, Tan Kean Giap, Abu-Ha Mohd Ariffin, Noor Zainura Zainon. Effect of fluidising velocity on the combustion of rice husk in a bench-scale fluidised bed combustor for the production of amorphous rice husk ash. *Bioresour Technol* 2008;99:703–13.
- [17] Lahijani Pooya, Zainal Zainal Alimuddin. Gasification of palm empty fruit bunch in a bubbling fluidized bed: A performance and agglomeration study. *Bioresour Technol* 2011;102(2):2068–76.
- [18] Chen Mao, Hou Xinmei, Chen Junhong, Zhao Baojun. Phase equilibria studies in the  $\text{SiO}_2\text{-}\text{K}_2\text{O}\text{-}\text{CaO}$  system. *Metall Mater Trans B* 2016;47(3):1690–6.
- [19] Broadley Sarah L, Plane John MC. A kinetic study of reactions of calcium-containing molecules with O and H atoms: implications for calcium chemistry in the upper atmosphere. *Phys Chem Chem Phys* 2010;12(31):9094–106.
- [20] Kim Dong-Geun, Konar Bikram, Jung In-Ho. Thermodynamic optimization of the  $\text{K}_2\text{O}\text{-}\text{Al}_2\text{O}_3\text{-}\text{SiO}_2$  system. *Ceram Int* 2018;44(14):16712–24.
- [21] Zhou Zhao-qiu, Ma Long-long, Yin Xiu-li, Wu Chuang-zhi, Huang Li-cheng, Wang Chu. Study on biomass circulation and gasification performance in a clapboard-typeinternal circulatingfluidized bed gasifier. *Biotechnol Adv* 2009;27:612–61.
- [22] Nisamaneenate Jurarat, Atong Duangduen, Sornkade Punchaluck, Sricharoenchaikul Viboon. Fuel gas production from peanut shell waste using a modular downdraft gasifier with the thermal integrated unit. *Renew Energy* 2015;79:45–50.